



Nanoscale

ARTICLE (Supporting Information)

Rapid Method for the Purification of Graphene Oxide (Supporting Information)

Gabriel Ceriotti,^a Anna Yu. Romanchuk,^b Alexander S. Slesarev,^a and Stepan N. Kalmykov^b

Perlite, Celite, polyester fibre, ceramic paper, glass wool, and woven glass fibre were tested as filterbeds in the enhanced filtration scheme described in the main text. As described in the main text, crude PGO could be optimally filtered with ceramic paper, while crude LFGO required a different filterbed. Both glass wool and woven glass fibre worked well for filtering crude LFGO, making it possible to filter 50 mL of the crude reaction mixture (1 g of precursor graphite equivalent) at 60 psi within 30 – 60 min. The only difference between glass wool and woven glass fibre is the ease with which woven glass fibre can be handled. Woven glass fibre was noted to be less likely to be incorrectly placed in the filter, and easier to recover. Separation of the filterbed and the filtercake was also harder with glass wool than with woven glass fibre. Similar issues were encountered when using perlite and Celite. Much of the Celite and perlite stays with the GO at the end of the process, and covering the funnel's porous plate unevenly, or using too little material for the filter bed can cause all or some of the sample to run through. The "running-through" problem can be alleviated by grinding the perlite or Celite until it goes through a 120 standard US mesh, but the filtration takes much longer. With ground perlite or Celite, 50 mL of crude LFGO would filter at 60 psi in 2 - 4 h. It was noted that the solid support, flocculants, or CaCO₃ needed in procedures 2, 3 and 4 do not always need to be removed. In applications such as enhancement of drilling fluids, or water purification it is possible to leave the GO with its associated purification support material.

Because of its tendency to create a very fluffy and porous filter, polyester fibre can be quite attractive as a filter bed for quenched crude LFGO. If the resulting flakes are large enough, a polyester fibre filter bed will retain most (or all) of the crude LFGO's flakes, and the filtration will be much faster than when using perlite, Celite, ceramic paper, glass wool, or woven glass fibre filter beds. However, polyester fibre dissolves readily in concentrated sulphuric acid, and will become mixed with the crude GO unless the crude sample has been previously quenched using H₂O and/or base. If polyester contamination in the sample is a concern, reducing the MnO₄⁻ in the quenched crude using H₂O₂ and increasing the pH of the suspension above 5 is recommended.

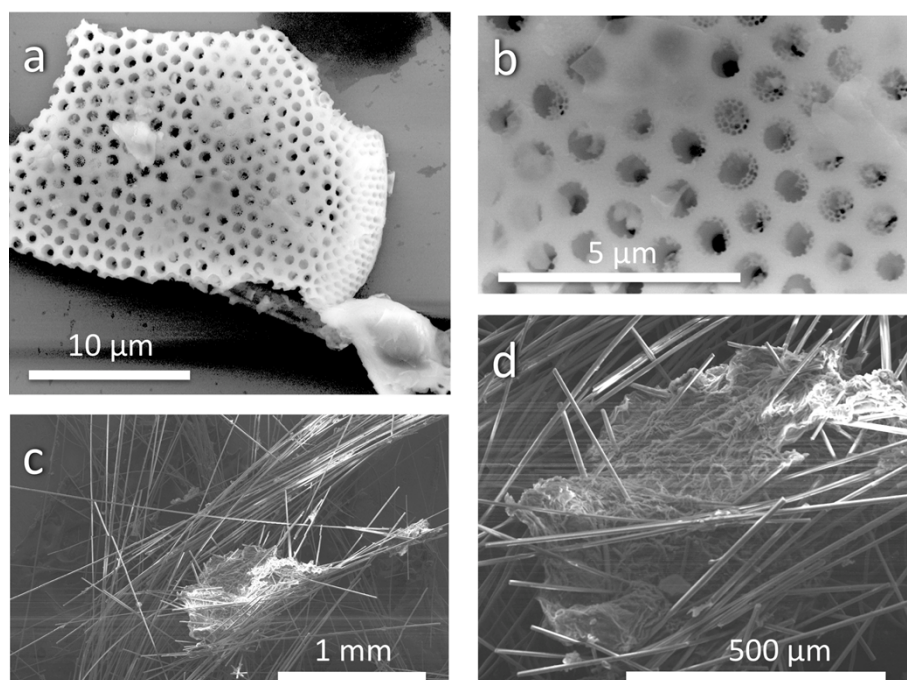


Figure SI-1. SEM images of (a, b) EPGO on Celite; and (c, d) ELFGO on glass wool.

Some of the materials used as solid supports for the filtration of crude LFGO (perlite, Celite, polyester fiber, and glass fiber) can also be used as precipitants. Mixing some of these materials in a suspension of crude LFGO will cause the nanoparticles to bottom-flocculate, and allow them to be decanted. Scanning electron micrographs of the LFGO aggregating onto Celite and glass fiber after bottom flocculation are shown in Figure SI-1. However, precipitating LFGO in this way did not enhance filtration. Additions of up to 6:1 w/w solid support/LFGO were attempted for filtration enhancement without any visible success.

The TGA of GOs (Figure SI-2a, b) shows inflection points at ~ 120 °C corresponding to evaporation of moisture from the very hygroscopic sample, and at ~ 200 °C corresponding to loss of the most liable oxygen groups. On occasion a sample might also exhibit an inflection ~ 400 °C attributed to the loss of sulfur-containing species, and at ~ 750 °C corresponding to the degradation of carbonates. This last band is to be specially expected when the sample contains potassium impurities. The presence of potassium might be an indication that potassium carbonate (or an analogous surface functionality) was formed during the process of synthesis, quenching, washing, or heating (as part of the TGA) of the sample. The ATR-FTIR spectra (Figure SI-2c, d) show qualitative and quantitative results that are in agreement with the analyses of the XPS C_{1s} peaks shown in Figure 5 of the main text.

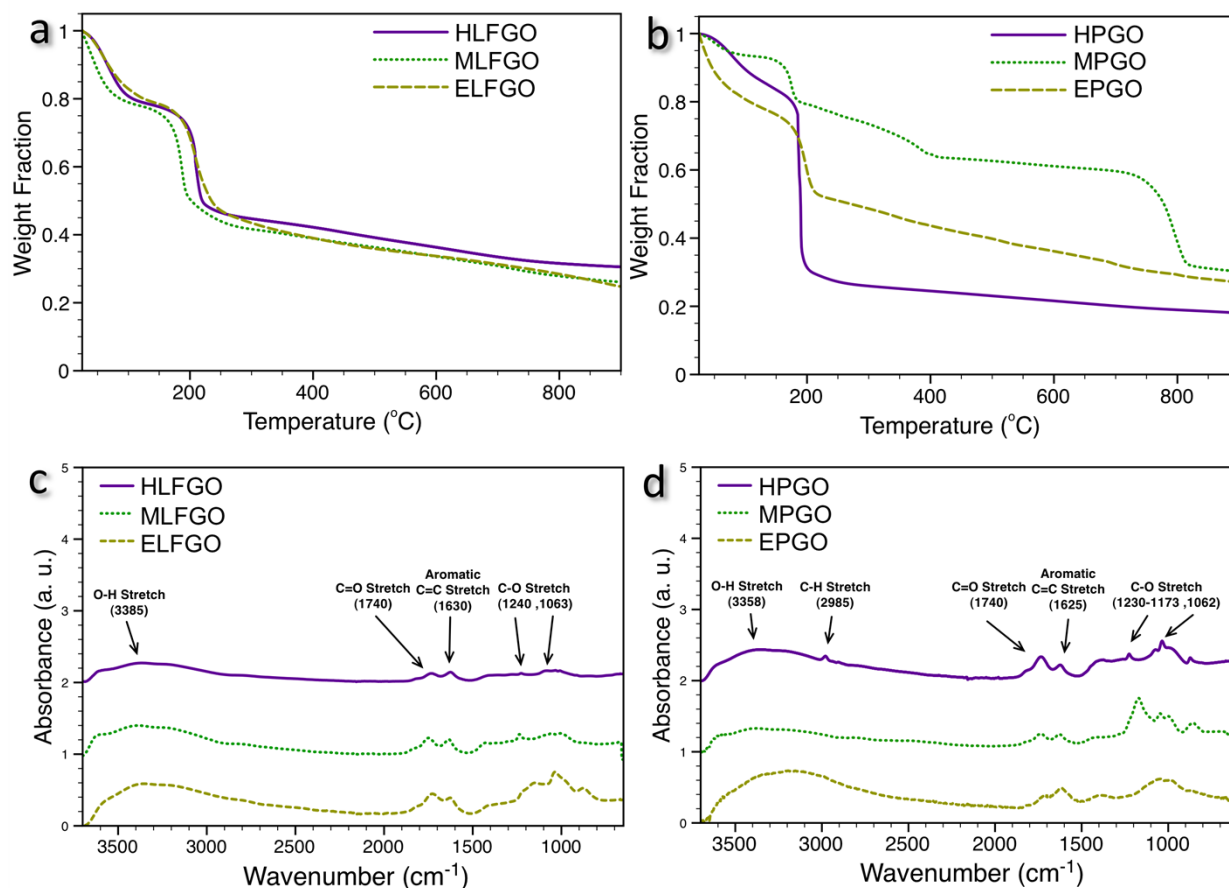


Figure SI-2. TGA of (a) LFGOs and (b) PGOs, and ATR-FTIR of (c) LFGOs and (d) PGOs.

The ATR-FTIR of differently purified crude PGO (Figure SI-3) shows how much the choice of solvent for filter-washing can affect the chemical characteristics of the final GO product. EPGO washed with 0.1 M NaOH exhibits stronger O-H stretch and C=O stretch bands and weaker C-O stretch bands. This is likely from the mild action of hydroxyl cations on the epoxy functionalities present in the GO whereby they are opened to give more hydroxyl functionalities. On the contrary, EPGO b filtered with a much more concentrated 1.0 M NaOH has already gone past the point of hydrolysis and lost oxygen functionalities to the strongly basic environment. Washing with either 10% HCl (EPGO c) or twice with DI H₂O (EPGO d) does not seem to significantly affect oxygen functionalities. On the other hand, washing with dilute HCl should facilitate the removal of manganese ions left from oxidation with KMnO₄, and washing with water makes the final pH of the purified GO closer to neutral. Washing with >10% HCl is not recommended as concentrated HCl seems to hydrolyze GO.

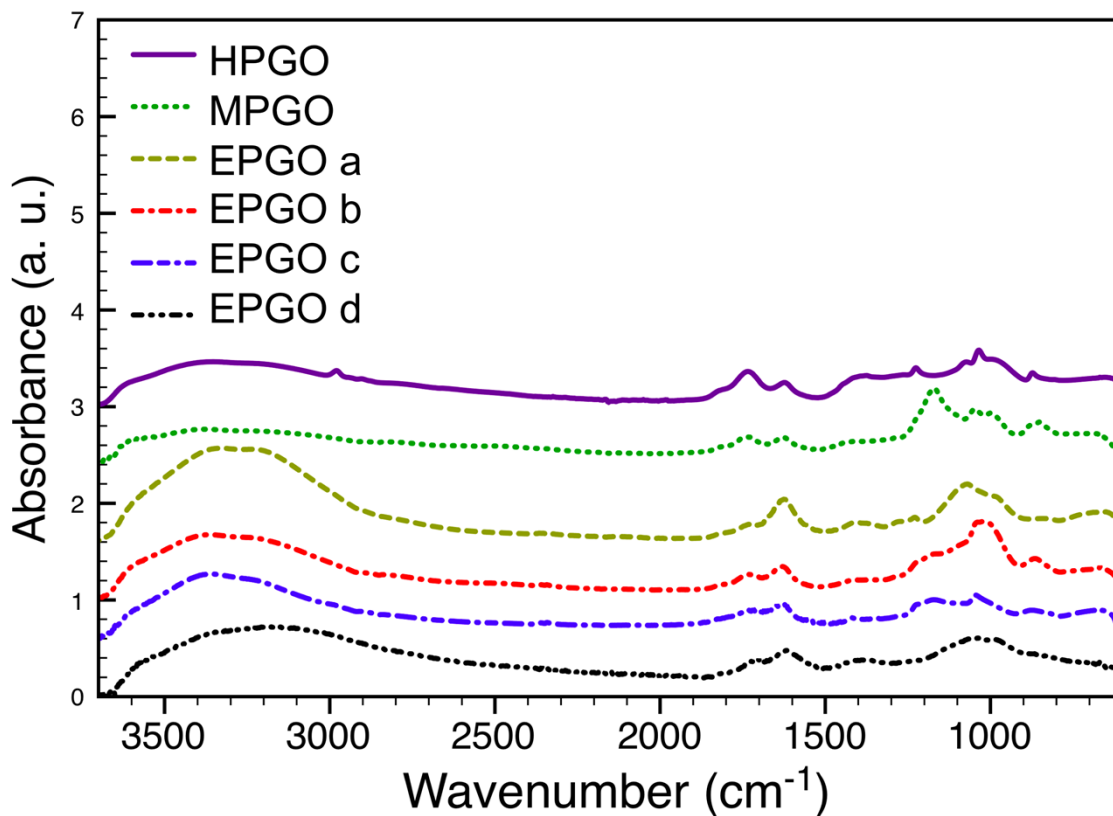


Figure SI-3. ATR-FTIR of HPGO (top purple), MPGO (green dotted line), EPGO a (olive dashed, produced by filter pressing on glass fiber paper with one 0.1 M NaOH wash), EPGO b (red dash-dot, produced by filter pressing on glass fiber paper with one 1.0 M NaOH wash), EPGO c (blue dash-dot, produced by filter pressing on glass fiber paper with one 10% HCl wash), and EPGO d (black dash-dot-dot, produced by filter pressing on glass fiber paper with two DI H₂O washes).

SO₄²⁻ coming from GO impurities could inhibit the adsorption of radionuclides. To test this, set concentrations were prepared as shown in Table SI-1. Additionally, the concentration of different aqueous radionuclide species at different pH and varying concentrations of SO₄²⁻ were computationally calculated by solving a set of state equilibrium equations for the system at pH 1 – 12. The results obtained are shown in Figure SI-4, and further details on the computation are given in the figure caption. As discussed in the main text, the drop in the pH-dependent sorption of U(VI), Am(III), and Ra(II) shown in Figure 8 of the main text coincides well with the increase in sulfate salt concentrations shown in Figure SI-4.

Table SI-1. Experimentally determined concentrations of aqueous SO_4^{2-} in HLFGO and ELFGO suspensions in deionized water with no additives.

	[GO] g/L	$[\text{SO}_4^{2-}]$ mg/kg	$[\text{SO}_4^{2-}]$ M
HLFGO	0.1292	200	0.002083333
ELFGO	0.051	186	0.0019375

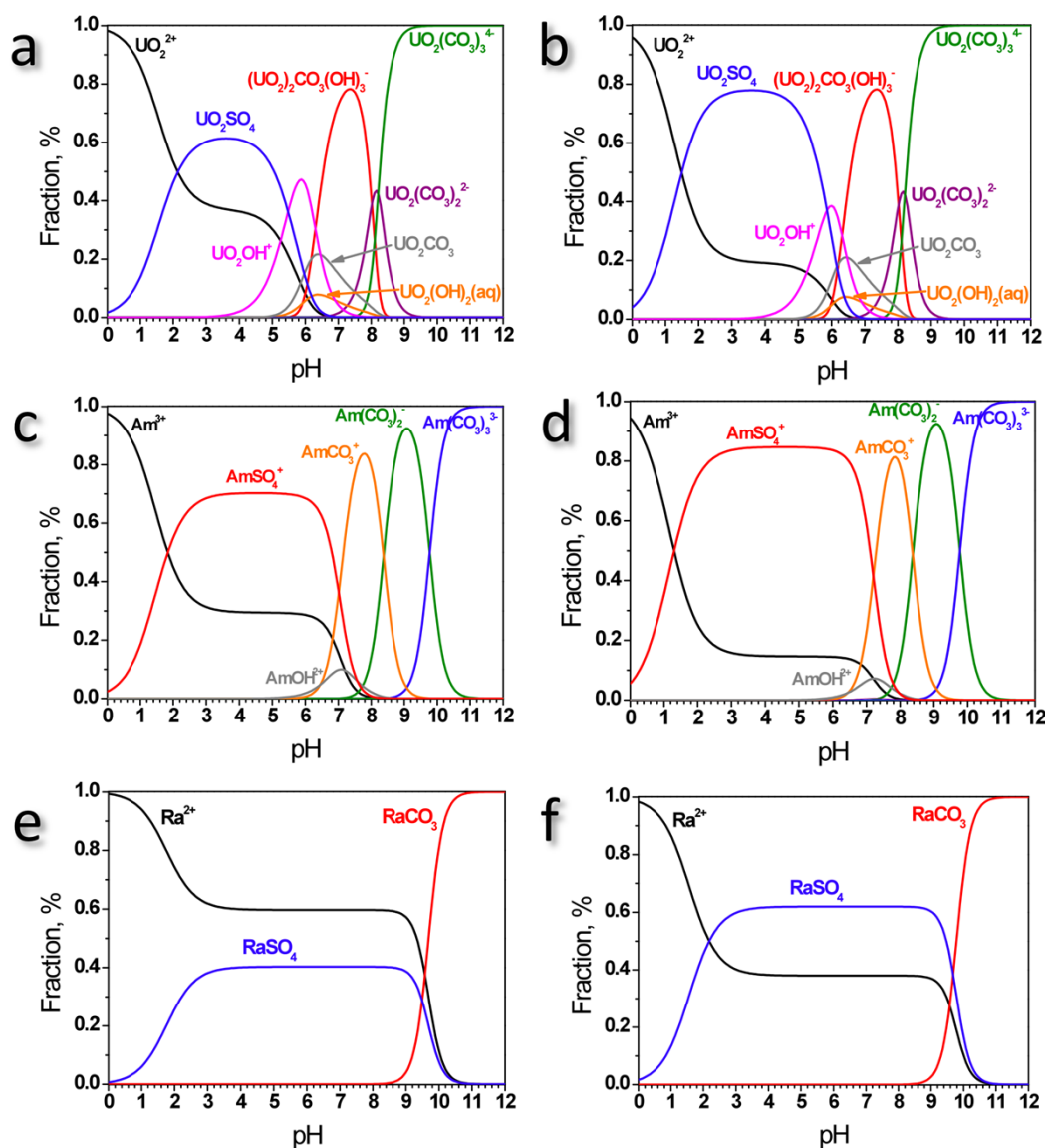


Figure SI-4. Computationally-derived speciation diagrams for U(VI)'s, Am(III)'s, and Ra(II)'s aqueous species in the presence of SO_4^{2-} at (a) $[\text{SO}_4^{2-}] = 0.0012 \text{ M}$ and (b) $[\text{SO}_4^{2-}] = 0.0029 \text{ M}$, with $[\text{U(VI)}] = 2 \cdot 10^{-7} \text{ M}$, and $\log P_{\text{CO}_2} = -3.5$, at (c) $[\text{SO}_4^{2-}] = 0.0012 \text{ M}$, and (d) $[\text{SO}_4^{2-}] = 0.0029 \text{ M}$, with $[\text{Am(III)}] = 4 \cdot 10^{-10} \text{ M}$, and $\log P_{\text{CO}_2} = -3.5$, and (e) $[\text{SO}_4^{2-}] = 0.0012 \text{ M}$, and (f) $[\text{SO}_4^{2-}] = 0.0029 \text{ M}$, with $[\text{Ra(II)}] = 4 \cdot 10^{-13} \text{ M}$, $\log P_{\text{CO}_2} = -3.5$. Sulfate concentrations are based on experimentally determined natural concentrations in HLFGO (a),(c),(e) and ELFGO (b),(d),(f) suspensions, reported in Table SI-1. Only the species with contribution of more than 5% are shown. Modeling was done using HYDRA¹ and MEDUSA² software and NEA thermodynamic data.^{3,4}

A detailed diagram of the gas-press filtration assembly is provided in Figure SI-5. It is believed that, with the information provided, a knowledgeable person could reproduce the in-house device used for this project. However, it should be noted that there currently are commercially available, acid resistant, lab-scale pressurized cylinder filtration assemblies that should be able to perform just as well (or better than) our in-house device.

Notes and references

^a Department of Chemistry, Rice University, 6100 Main Street, Houston, Texas, 77005, USA.

^b Department of Chemistry, Lomonosov Moscow State University, Leninskie Gory, Moscow 119991, Russia.

See DOI: 10.1039/b000000x/

- 1 Puigdomenech Hydrochemical Equilibrium-Constant Database, Royal Institute of Technology, Stockholm, Sweden, Vers. 2004
- 2 Puigdomenech Make Equilibrium Diagram Using Sophisticated Algorithms. Royal Institute of Technology, Stockholm, Sweden, Vers. 2004.
- 3 I. Grenthe, J. Fuger, R. Konings, R. Lemire, A. Muller, N. Nguyen-Trung Cregu and H. Wanner, Chemical Thermodynamics of Uranium. Nuclear Energy Agency, Organization For Economic Co-Operation And Development, 2004.
- 4 R. J.Silva, G. Bidoglio, M. H. Rand, P. B. Robouch, H. Wanner and I. Puigdomenech, Chemical Thermodynamics of Americium. Nuclear Energy Agency, Organization For Economic Co-Operation And Development, *Elsevier*, 2004.